




Layer-specific reduced neuronal density in the orbitofrontal cortex of older adults with obsessive–compulsive disorder

Katia Cristina de Oliveira^{1,2,3,11,13}  · Lea Tenenholz Grinberg^{1,12} · Marcelo Queiroz Hoexter² · Helena Brentani^{6,8,9} · Claudia Kimie Suemoto^{1,4} · Fabiano Gonçalves Nery³ · Luzia Carreira Lima¹ · Ana Tereza Di Lorenzo Alho^{1,10,11} · José Marcelo Farfel^{1,4} · Renata Eloah de Lucena Ferretti-Rebustini^{1,7} · Renata Elaine Paraizo Leite^{1,4} · Ariane Cristine Moretto^{1,3} · Alexandre Valotta da Silva^{1,10} · Beny Lafer^{3,9} · Eurípedes Constantino Miguel^{2,8,9} · Ricardo Nitri^{1,4,5} · Wilson Jacob-Filho^{1,4} · Helmut Heinsen^{1,11} · Carlos Augusto Pasqualucci^{1,13}

Received: 2 October 2017 / Accepted: 9 September 2018 / Published online: 8 October 2018
© Springer-Verlag GmbH Germany, part of Springer Nature 2018

Abstract

Neurobiological models have provided consistent evidence of the involvement of cortical–subcortical circuitry in obsessive–compulsive disorder (OCD). The orbitofrontal cortex (OFC), involved in motivation and emotional responses, is an important regulatory node within this circuitry. However, OFC abnormalities at the cellular level have so far not been studied. To address this question, we have recruited a total of seven senior individuals from the Sao Paulo Autopsy Services who were diagnosed with OCD after an extensive post-mortem clinical evaluation with their next of kin. Patients with cognitive impairment were excluded. The OCD cases were age- and sex-matched with 7 control cases and a total of 14 formalin-fixed, serially cut, and gallocyanin-stained hemispheres (7 subjects with OCD and 7 controls) were analyzed stereologically. We estimated laminar neuronal density, volume of the anteromedial (AM), medial orbitofrontal (MO), and anterolateral (AL) areas of the OFC. We found statistically significant layer- and region-specific lower neuron densities in our OCD cases that added to a deficit of 25% in AM and AL and to a deficit of 21% in MO, respectively. The volumes of the OFC areas were similar between the OCD and control groups. These results provide evidence of complex layer and region-specific neuronal deficits/loss in old OCD cases which could have a considerable impact on information processing within orbitofrontal regions and with afferent and efferent targets.

Keywords Human brain · Cerebral cortex · Cell count · Biomedical research · Obsessive–compulsive disorder · Obsessive–compulsive symptoms

Introduction

Obsessive–compulsive disorder (OCD) is a chronic disorder, characterized by recurrent intrusive thoughts and compulsive time-consuming behaviors. Worldwide, OCD prevalence is 2.5% in the general population and 1.5% in

noninstitutionalized older adults (Teachman 2007). The estimated direct and indirect costs of OCD are around 8.4 billion dollars per year in the US (DuPont et al. 1995). OCD will be the sixth most incapacitating disease worldwide by 2020 (Murray and AD 1996). Despite its undeniable burden, the pathophysiological basis of OCD is yet to be clarified.

Both structural and functional neuroimaging studies have indicated disturbances in cortico-striato-thalamo-cortical circuitry (CSTC) as a possible mechanism underlying OCD symptoms (Rauch et al. 1994a; Subira et al. 2016). Among the structures involved in this circuitry, abnormalities in the orbitofrontal cortex (OFC) have been one of the most consistent findings in neuroimaging studies of OCD patients (Hoexter et al. 2015). However, current evidence is controversial. Structural imaging studies comparing OCD patients and controls reported greater OFC gray matter volume

Presented at the Alzheimer’s Association International in Copenhagen, Denmark, from July 12 to 17, 2014.

Electronic supplementary material The online version of this article (<https://doi.org/10.1007/s00429-018-1752-8>) contains supplementary material, which is available to authorized users.

✉ Katia Cristina de Oliveira
katia.oliveira@pq.cnpq.br

Extended author information available on the last page of the article

(Christian et al. 2008; Kim et al. 2001; Valente et al. 2005), while others showed a reduction (Hoexter et al. 2012; Pujol et al. 2004; Rotge et al. 2010; Szeszko et al. 1999; Togao et al. 2010; Yoo et al. 2008). Functional imaging studies have shown similarly conflicting results, since both hyperactivation (Gillan et al. 2015; Harrison et al. 2012; Maltby et al. 2005) and hypoactivation (Chamberlain et al. 2008) of the OFC areas were reported. Several factors could have contributed to these uncertainties, such as different imaging techniques and heterogeneity in OCD clinical presentation.

The human OFC is subdivided into areas or regions with distinct cytoarchitecture and hodology (Beck 1949; Brodmann 1909; Economo and Koskinas 1925; Hof et al. 1995; Mackey and Petrides 2010; Sanides 1962; Uylings et al. 2010; Vogt and Vogt 1919; Ongur et al. 2003). In addition, the main regions of the OFC, particularly the medial orbitofrontal (MO), anterolateral (AL) and anteromedial (AM), may have distinct roles (Chamberlain et al. 2008; Milad and Rauch 2007, 2012). For this reason, we focused onto these three important regions in our study.

Neuropathological examination of post-mortem brains is the gold standard method to assess the clinicopathological basis of diseases, including dementia, movement disorders and stroke. For example, in Alzheimer's disease, specific protein accumulation, such as tau phosphorylation and amyloid beta, were detected and are used as diagnostic evidence (Braak and Braak 1991). In the case of OCD, to date, no specific neuropathological lesion has been recognized in post-mortem brain examinations.

Stereology is the method of choice for assessing neuronal number and volume. It requires the availability of the whole regions of interest, as well as the unified random selection of fields under stereologic analysis (Schmitz and Hof 2005). These requirements pose limitations because entire brains of well-characterized OCD patients are rarely available. For this reason, very few neuropathological or morphometric post-mortem studies of psychiatric disorders have been performed, and none of them has been conducted on OCD (Beasley et al. 2005; Cotter et al. 2005; Law and Harrison 2003; Pakkenberg 1990; Rajkowska et al. 2001; Stockmeier et al. 2004; Todtenkopf et al. 2005). Therefore, we applied unbiased stereological tools to estimate post-mortem neuronal density and volume, within OFC areas to achieve a clearer understanding of the neurobiological basis of OCD.

Materials and methods

Ethics statements

The brains studied herein were part of the psychiatric disorders collection of the Brain Bank of the Brazilian Aging Brain Study Group (Psy-BBBABSG). They were sourced

from the Autopsy Service of the University of São Paulo between 2009 and 2011 (de Oliveira et al. 2012). All protocols concerning the acquisition of data and tissue processing were approved by the Research Ethics Committees of the University of São Paulo Medical School (Process number: 740/09), and by the Brazilian National Commission of Research Ethics (CONEP, Process number: 540/09) and are in accordance of The Code of Ethics of the World Medical Association (Declaration of Helsinki). The informed consent was obtained from all individual participants included in this research.

Participants

We analyzed 14 hemispheres (7 with OCD and 7 controls) from subjects who were ≥ 50 years old and without signs of clinical dementia at the time of death. Control cases were selected to match to the OCD group, regarding post-mortem interval (PMI), cerebrospinal fluid pH (CSF pH), age, sex, and hemisphere analyzed. Further detailed information concerning our collection is discussed elsewhere (de Oliveira et al. 2012).

Clinical assessment

After signing a term of free informed consent, the deceased's next of kin (NOK) answered a comprehensive interview on clinical, functional, cognitive and psychiatric information (Ferretti et al. 2010). In participants with a presumable diagnosis of OCD during the screening interview, we invited the NOK to return for a second interview, with an experienced psychiatrist for confirmation of OCD diagnosis. This complete evaluation comprised a Structured Clinical Interview for DSM IV Axis I disorder (SCID) (Del-Ben et al. 1996; First et al. 2002; Spitzer et al. 1992), the Yale–Brow Obsessive–Compulsive Scale (Y-BOCS) (Goodman et al. 1989), and a short version of DY-BOCS (Rosario-Campos et al. 2006). We considered a cutoff ≥ 1 for the Neuropsychiatry Inventory score.

It is relevant to note that none of the subjects diagnosed with OCD post-mortem has received a diagnosis of OCD during their lives.

Histological processing

After removal from the skull, the brains were subdivided by a medio-sagittal cut. One hemisphere was dissected fresh into 46 blocks and frozen for future studies. The contralateral hemisphere was perfusion-fixed with formalin at 20% and post fixed for at least 3 months. After fixation, the brain tissue was dehydrated and embedded in celloidin. The blocks were cut along the coronal axis using a sliding microtome

(Polycut, Cambridge Instruments, UK), producing serial sections of 440 μm thickness.

Photograph image acquisition

A monopod with a digital camera (Canon EOS 5D Mark II 21.1 Megapixel[®], Tokyo, Japan) was firmly attached to the microtome knife holder, allowing each section to be photographed while the block was cut. These images were used for computer-assisted three-dimensional (3D) reconstruction of all frontal lobes, using Amira software (FEI, ThermoFisher Scientific) 3D reconstruction was mandatory for architectonic evaluation of the regions of interest.

Odd-numbered sections were stored in 70% alcohol and representative planes of sections were used to perform the neuropathological examination for Alzheimer's disease, according to The Consortium to Establish a Registry for Alzheimer's Disease (CERAD) (Mirra et al. 1991) criteria and Braak and Braak staging (Braak and Braak 1991). All even-numbered serial sections were stained with galloycyanin (Einarson 1932) and photographed at low magnification, using a digital single-lens reflex camera (Canon EOS 5D Mark II 21.1 Megapixel[®], Tokyo, Japan) mounted with a 1:2:8/90 mm macro lens (Vivitar[®], Tokyo, Japan). Moreover, a wide-field stereomicroscope (Olympus[®], Tokyo, Japan) with zoom lenses ranging in magnification from 5 to 120 \times was used to delineate the cytoarchitectonic fields on the Nissl-stained sections and to draw the boundaries of the orbitofrontal areas AM, MO and AL (Heinsen et al. 1999).

Cytoarchitectonic delineation

The criteria for cytoarchitectonic delineation included: absolute cortical thickness and relative thickness of the cortical layers I through VI in corresponding locations in the gyri, relative thickness of the combined layers I through IV versus layers V + VI, size, staining properties, and cell densities of pyramidal cells in layers IIIc and V, subdivision of layer V into Va and Vb; presence, thickness, and granule cell density of layer IV, and thickness, and sharpness of cortical to subcortical border of layer VI. For parcellation of the orbitofrontal cortex, we were using the terminology of Hof et al. (1995).

The anterior borders of AM, MO, and AL are formed by the frontopolar region, characterized by a high thickness of layer IV and high cell number of granule cells (Fig. 1a, b). The caudal border of AL was set at the transition of the granular orbitofrontal area AL to the dys- or agranular part of the lateral orbital gyrus, the continuation of the inferior frontal gyrus (Fig 1a, d, e, F3o) (Eberstaller 1890; Economo and Koskinas 1925). Sagittal sections represent the standard plane of section for anterior–posterior delineation of rostro-caudally arranged cytoarchitectonic fields. However, neither

the anterior nor the caudal borders were sharply delimited at low-power magnification (Fig. 1a). Furthermore, we have excluded region PM from our study, because the delineation of granular- and dysgranular areas in coronal sections was subject to considerable interindividual variability between researchers involved in delineation. The same was true for the frontopolar delineation. There was an area of transition (Fig. 1a) between the frontopolar regions and the ensuing caudal orbitofrontal fields and particularly the increasing number of layer IV granule cells made the delineation of MO and AL uncertain in coronal sections. According to Hof et al. (1995) AM covers the depth of the olfactory sulcus and also the ventral part of the rectus gyrus. We had set the medial border of AM into the olfactory sulcus, because in 5 out of our 14 cases the rectus gyrus was artifactually lesioned and a cytoarchitectonic delineation of the complete AM was not possible. The medio-lateral delineation of fields AM, MO, and AL was less ambiguous because the borders were always in the same plane of our coronal sections.

Stereological estimations

Neuronal density is not homogeneous but subject to gradual caudo-rostral increase in layers II through VI (Fig. 1a). After 3D-reconstruction of the cytoarchitectonic fields AM, MO, and AL, we selected coronal planes of section midway between the presumptive rostral and caudal borders of the fields. We placed a transparent folia printed with a 1 \times 1 mm grid over the serial sections and selected those crossing points hitting representative and undistorted sections through the dome (crown), wall, fundus or sulcal floor (Triarhou 2013) of AM, MO, and AL. To eliminate bias caused by tangential sections, only crossing points hitting perpendicular sections through complete gyral profiles were selected. Neuron densities were determined along a virtual perpendicular line through the crossing point within layers IIIa, IIIb, IIIc, IV, Va, Vb, VIa, and VIb in the dome, wall, and floor regions, summarized and divided by three (mean of each layer of the three representative regions of a gyrus).

We estimated neuron density using the unbiased optical disector. Each cortical layer of the area was counted separately. In each cortical layer, the disector height was set to 30 μm and the guard zone to 15 μm (Heinsen et al. 1999). We took serial images of optical stacks comprising 11 pictures, focusing within the z-axis of the microscope by turning the fine adjustment knob (within a range of 30 μm). The microscope's lens was a PlanApo40/1.0 oil and the photographic ocular a FK 5 \times . The stack of virtual images was imported to the cell counter plugin of the Image J 1.45I software (National Institutes of Mental Health, EUA). The final magnification on the computer screen was 1500-fold. Scrolling through the optical stack is like virtual focusing through galloycyanin stained neurons. All profiles of neuronal

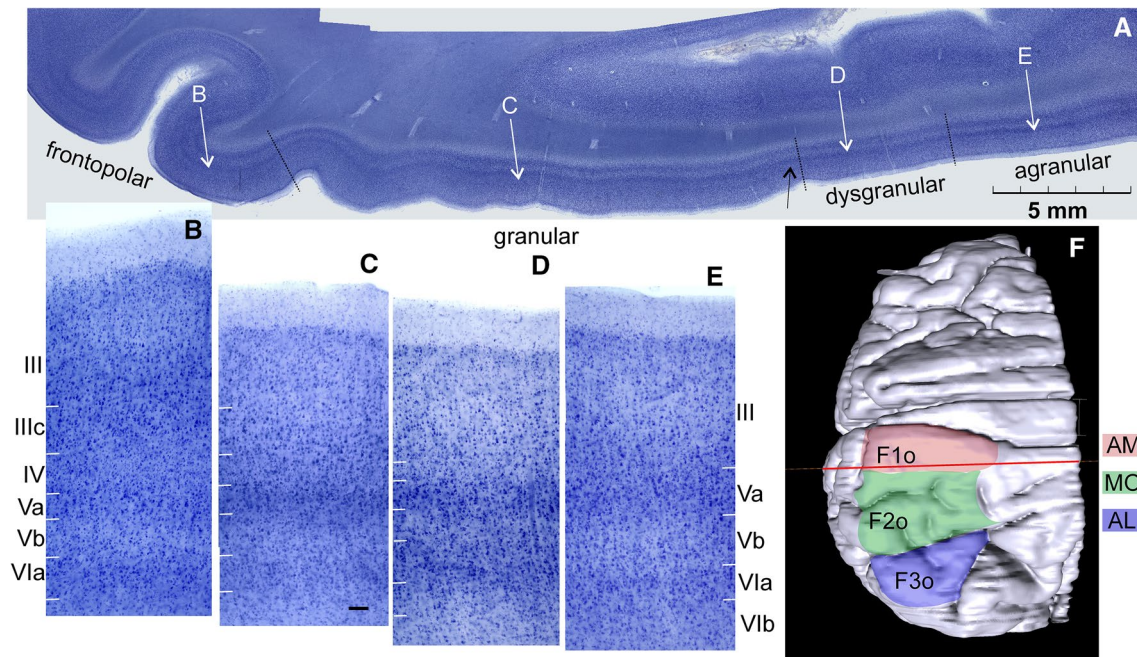


Fig. 1 Sagittal section through the right orbitofrontal cortex of a 68-year-old female control case. The plane of section is indicated by the red line in **f**. The low power overview clearly demonstrates postero-anterior changes in laminar width and staining properties of layers III through VI. Layer V is prominent in the posterior orbital part of the superior frontal gyrus (F1) and sublayer Va is characterized by is strong staining (chromophilia) with gallocyanin and Vb by its palor due to a relatively low overall cell density. This chromophilia is decreasing in the anterior (rostral) direction and the superior and inferior borders of layer Va become blurred whereas the cell density in increasing in Vb to reach a maximum in the frontopolar region. The granule cells of layer IV are small, round, and less-well stained with gallocyanin, layer IV is interspersed between layers III and V. It is missing in posterior (agranular) fields of F1, barely recognizable in the dysgranular fields, and it becomes more prominent and reaches a

maximum in width and cell density in the frontopolar region or area 10 of Brodmann. Black arrow marks an emergent layer IV, black bar in lower-right, 100 μm , same magnification in all microscopic pictures (**b–e**); white arrows and letters indicate the position of figures **b** through **e** at higher microscopic magnification. **f** Computer-assisted reconstruction of the orbitofrontal regions AM (anteromedial), MO (medial orbitofrontal), and AL (anterolateral) according to Hof et al. (1995). F1o, F2o, F3o continuation of the superior (F1), medial (F2), and inferior frontal gyri (F3) into the orbital region based on the terminology of Economo and Koskinas (1925). The lateral parts of F1o correspond to the medial orbital gyrus, the rostral parts of F2o to the anterior, the posterior parts of F2o to the posterior orbital gyrus, and F3o to the lateral orbital gyrus of Chiavaras and Petrides (2000) respectively

nucleoli that came anew onto the computer screen were counted. Nucleoli in granule cell nuclei could not always be identified or could be confused with larger clumps of heterochromatin. In this case, profiles of granule cell nuclei coming anew into the field of focus were counted. We have never observed neurons with more than one nucleolus per cell. The area of the counting frame was $80 \times 80 \mu\text{m}$ or 0.0064 mm^2 . We set the left and the lower margin as forbidden lines. The neuronal density (N) was calculated according to the formula (1):

$$Nv = N/A \times t, \quad (1)$$

where N is the number of nucleoli counted, A is the area of the frame (0.0064 mm^2) and t is the optical thickness ($30 \mu\text{m}$ or 0.03 mm). For volume estimation, digital photos of all slices of the OFC were imported into Image J. A virtual grid with $d=0.7 \text{ mm}$ was randomly overlaid on each slice. All

crossing points that hit the region of interest were counted. Then volume (V) was calculated using the Cavalieri principle (West 1999), according to the formula (2):

$$V = k \times d^2 \times t \times P_T, \quad (2)$$

where k was the distance between sections (2, since we had stained every second section), d^2 was the area of the grid associated with each crossing point (P) (Weibel 1979) of the counting grid ($0.7 \times 0.7 = 0.49 \text{ mm}^2$) P_T is the sum of the crossing points counted for all sections, and t was the mean thickness of the hemispheric sections ($\approx 0.4 \text{ mm}$).

The precision and effectiveness of counting is a matter of debate (Schmitz 1997, 1998, 2000; Schmitz and Hof 2000, 2005; Schmitz et al. 1999a, b). In analogy with Schmitz (1998) recommendations we have counted between 671 and 2239 neurons per case to reduce the methodological error associated with sampling and counting procedures to $\approx 5\%$.

Statistical analysis

We described the variables of interest using means and standard deviations for continuous variables, and absolute and relative frequencies for categorical variables. We used Fisher's exact test to compare categorical variables between control and OCD groups, and the Mann–Whitney test to compare continuous variables. For all tests, the significance level was set at 0.05. We used Stata 13.0 software (College Station, TX: StataCorp LP) for statistical analysis.

Results

Participants

Seven subjects who had OCD and seven matched controls were selected. The inspection of each brain showed no significant difference between OCD and control subjects regarding macroscopic neuropathological lesions, such as infarcts. However, we observed of tau and a amyloid-beta pathology in two candidates (one case and one control), based on CERAD criteria (Table S1).

OCD clinical presentation of cases, as reported by the NOK, is presented in Table 1. As expected, the groups were similar regarding variables used to paired participants (i.e. age, sex, hemisphere analyzed, PMI, and cerebrospinal fluid pH) (Table S2). Groups were also similar for other important variables, such as education level, smoking and alcohol use. The Neuropsychiatry Inventory (NPI) score and SCID were negative in the control group.

Qualitative differences between control and OCD cases

In general, perfusion fixation of hemispheres from controls and cases with short post-mortem time and with controlled CSF-pH resulted in excellent preservation of neuronal size, shape, and Nissl substance. Preservation of subcortical gray matter was not always optimal and most likely the consequence of intravascular blood clotting and limited flow of formalin. With low power magnification, the caudo-rostral and medio-lateral gradation in layer width, number and intensity of staining did not show pathognomonic differences between controls and the OCD cases (Figs. 1a, 2a). Applying the criteria described in “Material and methods”.

AM, MO, and AL could be unequivocally delineated from each other medio-laterally. However, the anterior borders with the frontopolar field and the posterior borders with dysgranular fields were less sharp and barely visible in coronal sections. These central parts of AM, MO, and Al comprised a minimal number of 10 and a maximal number of 17 serially cut slices with uncertain rostral and caudal boundaries.

With higher magnification, we became aware of local or extended lower cell densities in cases with OCD (Figs. 2b–d, 3b–d). These figures should be viewed from a considerable distance to blur neuronal details. Irregularly shaped paler regions will become visible in different layers after this maneuver. Uniform laminar differences in neuron density were more difficult to diagnose macroscopically (Figs. 2a, 3a). Laminar or focal pallor in the

Table 1 Description of obsessive–compulsive symptoms of the OCD patients

Sample ID	OCD symptoms
OCD1	He washed objects and hands excessively (10–12 times per day, each washing used to take at least 10 min). He took long baths and worried about dirt. Every morning, he had to count the seats before sitting down. He also had motor tics
OCD2	He stored plastic bags. He had his own dishes and would not share them with other members of his family. He washed his dishes many times until they became shiny, sometimes hurting his hands. No one but him could wash his dishes. The patient was a smoker 50 years ago, and had a history of treatment for alcoholism 18 years ago
OCD3	He presented compulsions that involved organizing clothes and newspapers. He also used to accumulate newspapers
OCD4	He had to arrange objects the “right” way and it had to be “perfect”, otherwise he became very anxious. He also had a collection of useless objects on a shelf in the service area. He did not allow anyone to touch them. If that happened, he became nervous
OCD5	She had to organize objects in a specific way and she did not let other people change the way these objects were arranged. She also kept useless objects throughout her life and these objects had to be stored always in the same place and in the right position. She could not stand throwing away or storing these objects in different places
OCD6	He wore the same clothes many times to prevent “bad things” from happening. He locked all closets with padlocks to avoid other people from moving or arranging his things. Every day and many times, he had to check and recheck whether the padlocks were locked. He used to bring home old things that he had found in the street. He kept expired medications and useless broken objects
OCD7	She had several superstitious behaviors, such as seeing a black cat as a sign of bad luck and not walking under a ladder. She collected useless objects (bottles, old things, books, knickknacks) and no one could touch them. She had to organize these objects in the “right” manner, maintaining a specific sequence of ordering them. Some of the collected objects were kept to be recycled at some point

OCD obsessive–compulsive disorders

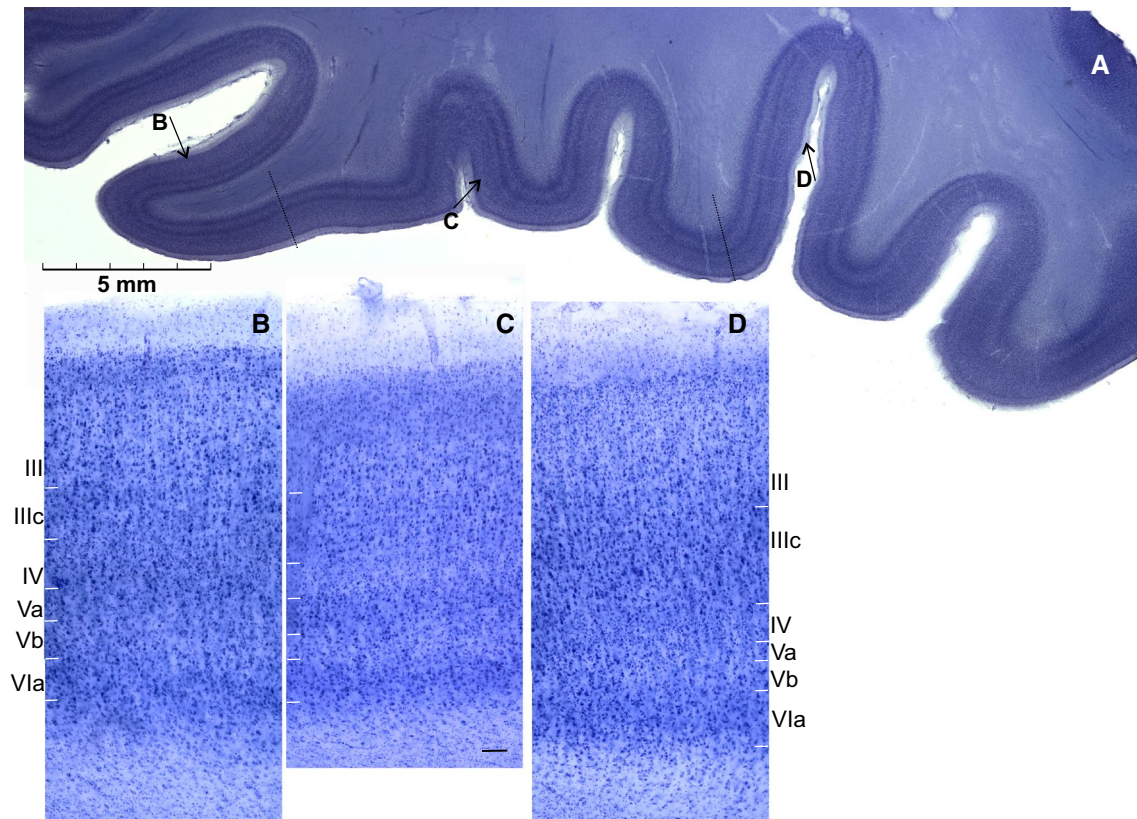


Fig. 2 **a** Coronal section through the right orbitofrontal cortex of a 71-year-old male control case. From the medial (left) to lateral (right) margin of the orbitofrontal cortex a similar layer-wise gradation concerning chromophilia, increase in neuron density, and changes in absolute and relative width of layers III through VI as in Fig. 1a can be observed. Latero-medial increase in depth and increase in granule cell number parallels an increase in width of layer III and particular increase in the number and size of deep IIIc pyramidal cells are main

characteristics of this medio-lateral gradation, whereas the size and staining intensity of layer V pyramidal cell decreases. Black arrows indicate the position of figures **b** through **d** at higher microscopic magnification. **b** anteromedial region; **c** medial orbitofrontal region; **d** anterolateral region. Black bar lower right of **c** 100 µm. Stippled lines from left to right cytoarchitectonic borders between AM/MO and MO/AL

cortical gray matter can be the result of neuron loss that can be quantified and subjected to statistical analyses.

Neuron density and areal cortical volume in OCD and controls

Our quantitative estimation of neuron densities confirmed the qualitative impression of reduced total neuronal densities (Table 2) ranging from –25% in AM and AL and –21% in MO. However, there was no consistent trend of a layer-specific decrease in all three OFC fields analyzed. Numerically, the infragranular layers were most heavily affected in all three fields, the supragranular layer IIIb particularly in AM and MO of the OCD cases. The mean volume of the combined areas was slightly but not significantly lower in our OCD cases (Table 3).

Discussion

To our knowledge, this is the first cytoarchitectonic study that includes estimation of neuronal density and volume of defined OFC-regions in post-mortem brains of subjects with OCD. Cytoarchitectonic delineation of the human orbitofrontal cortex was subject of numerous investigators and the results were not always uniform [for a recent summary and review see (Henssen et al. 2016)]. Nevertheless, we succeeded in subdividing the central orbitofrontal regions into three medio-lateral fields that correspond to subdivisions described previously by authors using combined Nissl and immunohistochemical stains (Ongur et al. 2003; Uylings et al. 2010) or sophisticated image analysis (Henssen et al. 2016). Our field AL did not extend into polar regions like the one depicted by Hof et al. (1995).

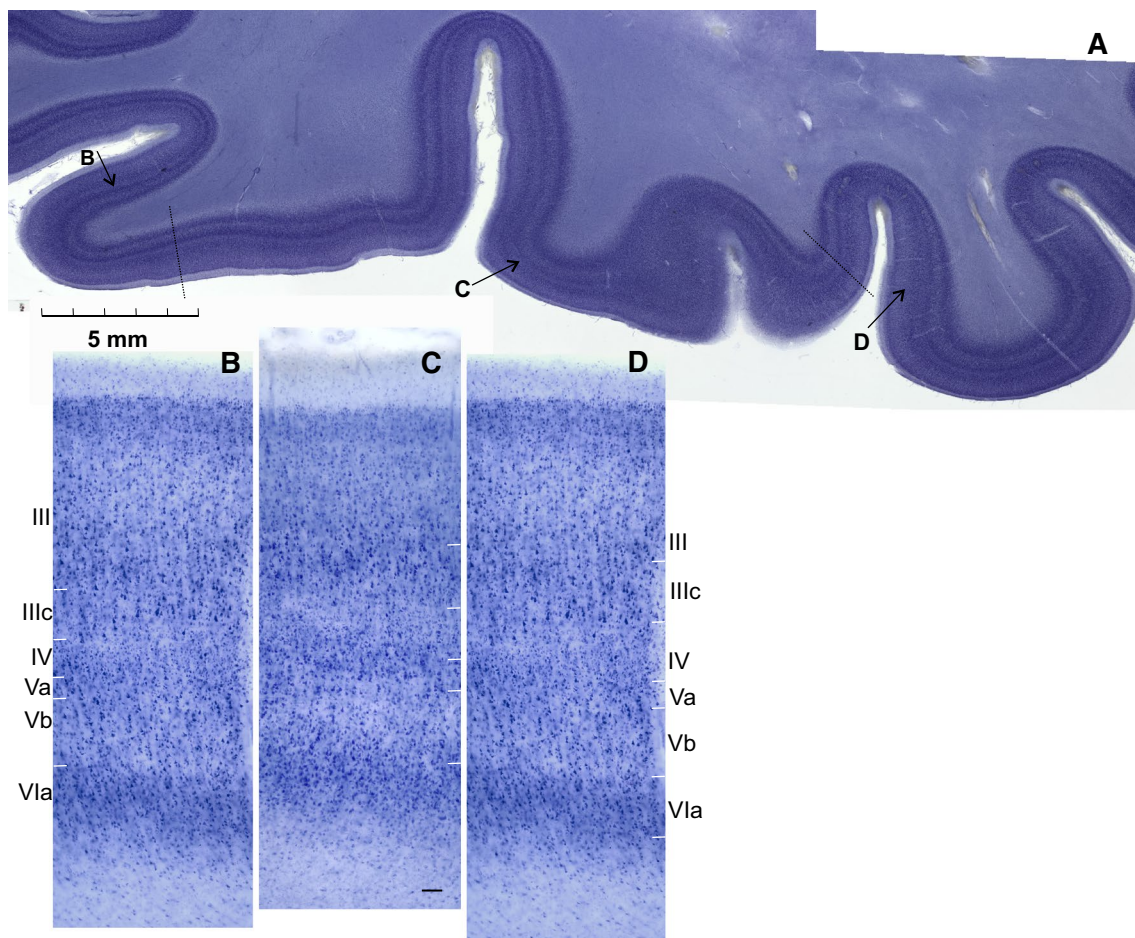


Fig. 3 **a** Coronal section through the left orbitofrontal cortex of a 66-year-old female OCD case. The overall cell density in all three regions (**b** anteromedial; **c** medial orbitofrontal; **d** anterolateral) is lower than in the control case, the presence of hyperchromic and large IIIc pyramidal cells and the columnar (vertical) arrangement of neu-

rons is striking. The latter phenomenon is masked in Fig. 2 by higher overall cell density. Black arrows indicate the position of figures **b** through **d** at higher microscopic magnification. Black bar lower right of **c**, 100 μm . Stippled lines from left to right cytoarchitectonic borders between AM/MO and MO/AL

Subtle architectonic differences between AL and FP after SMI-32 immunohistochemical staining could explain this discrepancy. We observed a puzzling non-uniform decrease of laminar neuron densities in OCD versus age- and sex-matched control cases. The greatest quantitative differences were more frequently encountered in the infragranular layers, whereas layer IIIb appeared particularly vulnerable in AM. Granule cell density in layer IV seemed to be unaffected.

Differences in neuron density can be artefactual and simply reflect less shrinkage in individual brains during fixation, embedding, staining, and coverslipping (Heinsen et al. 1994; Oorschot 1994). Multiplication of neuron density with the volume of a cytoarchitectonic field yields total neuron number, a dimension that is not biased by histological artifacts. However, we had exclusively estimated laminar neuron density in the sulcal depth, the wall and the crown in central regions of the orbitofrontal cortex. This procedure

does not reflect the relative volumes of cortical layers and the high neuron density of the thin layers IV or Va will automatically bias calculations of mean cortical neuron densities. Consequently, multiplication of our mean cortical neuron densities with the volume of the cortical fields estimated by the Cavalieri principle will necessarily yield biased total areal neuron numbers with little biological significance. Our primary focus was on the analysis of laminar neuron densities. This is only possible in strictly perpendicular sections through the cortex, whereas unbiased total neuron number must also be estimated in grazing or tangential sections of a cortex as well, depending on the random location of a hitting point (see Fig. 1a where laminar diagnosis in several profiles of the cortex dorsal to the more or less perpendicularly cut ventral cortex is illusive). On the other hand, selective regional differences in laminar neuron densities provide a strong argument against artifact-induced swelling associated with decreased neuron density and the impression of

Table 2 Comparison of the neuron density (N/mm³) in the cortical layers between OCS and controls

Area	Layer	OCS (<i>n</i> =7), mean (SD)	Control (<i>n</i> =7), mean (SD)	<i>p</i> * value
AM	IIIa	36,614 (6016)	47,831 (11,851)	0.048
	IIIb	27,937 (5180)	41,085 (12,850)	0.005
	IIIc	29,418 (6368)	40,847 (9840)	0.018
	IV	43,915 (9721)	55,979 (15,625)	0.110
	Va	35,979 (5147)	49,418 (13,277)	0.013
	Vb	30,688 (7393)	39,682 (12,914)	0.179
	VIa	33,122 (2483)	42,011 (9636)	0.006
	VIb	26,349 (5985)	36,190 (14,823)	0.055
AM total		33,003 (5175)	44,127 (11,846)	0.181
MO	IIIa	41,799 (9552)	49,100 (13,427)	0.277
	IIIb	29,974 (4379)	40,847 (11,270)	0.015
	IIIc	31,852 (5203)	41,587 (9970)	0.035
	IV	43,810 (8287)	53,439 (14,718)	0.124
	Va	41,481 (7816)	50,900 (15,949)	0.337
	Vb	33,968 (3739)	44,762 (10,818)	0.008
	VIa	34,180 (4474)	45,503 (11,703)	0.015
	VIb	28,677 (4206)	37,460 (11,640)	0.030
MO total		35,714 (3719)	45,450 (11,501)	0.030
AL	IIIa	40,212 (12,856)	48,677 (11,834)	0.063
	IIIb	30,265 (6576)	41,799 (11,935)	0.053
	IIIc	30,688 (5736)	41,164 (9816)	0.021
	IV	44,550 (10,124)	49,418 (13,783)	0.442
	Va	36,402 (7703)	54,391 (17,864)	0.018
	Vb	33,016 (6136)	44,339 (15,068)	0.072
	VIa	33,968 (4112)	46,243 (9368)	0.006
	VIb	25,397 (5455)	38,201 (12,907)	0.009
AL total		34,312 (5274)	45,529 (11,686)	0.047

OCS obsessive compulsive symptoms, SD standard deviation, AM anterior medial, MO medial orbitofrontal, AL anterior lateral

*Mann–Whitney test

Table 3 Comparison of the volume, between OCD subjects and controls

Variable	Area	OCS (<i>n</i> =7), mean (SD)	Control (<i>n</i> =7), mean (SD)	<i>p</i> value
Volume (V)	AM	391.7 (32.6)	364.7 (52.6)	0.75
	MO	536.7 (45.1)	595.6 (57.0)	0.65
	AL	429.5 (44.7)	489.2 (50.5)	0.52

AM anterior medial, MO medial orbitofrontal, AL anterior lateral, SD standard deviation

neuron loss. Artifact-associated histological procedures were reported to affect cortex and white matter in a more comprehensive or global way (Kretschmann et al. 1982). Finally, enhanced or reduced neuron density does not necessarily imply higher total or reduced neuron number respectively. We have recently reported a circumscribed laminar neuronal loss and overall decreased neuron number in Huntington's

disease in the presence of higher average neuron density associated with global cerebral atrophy and a reduced neuron number with massive gliosis and unchanged average cortical volume in chorea-acanthocytosis, an extremely rare disease with clinical symptoms similar to Huntington's disease (Liu et al. 2018).

Nevertheless, the average neuron density was by 21–25% lower in the OCD cases. Comparing b–d in Figs. 2 and 3 reveals a selective deficit or loss of smaller pyramidal neurons in OCD cases with preservation of bigger, particularly layer IIIc and chromophilic Vb neurons. Neuron loss by degeneration, neuronal deficits due to maldevelopment, or age-related proliferation with hypertrophic plasticity of the neuropil in the orbitofrontal cortex need to be verified as a pathogenetic mechanism behind diffuse and/or localized laminar pallor in Nissl-stained sections. Indeed, whereas we found a non-significant slight volume decrease in our sample (not corrected with individual shrinkage factors) (Heinsen et al. 1994; Oorschot 1994). de Wit et al (2014) describe

complex local group-by-age interactions with a relative preservation of orbitofrontal cortical volumes comprising area 13 and 47 (parts of our MO) in aged OCD. Their data are based on an international voxel-based morphometric *in vivo* 1.5 T T1-weighted MRI study on 412 OCD patients and 368 control cases. Given decreased neuron density reflects decreased neuron number, a relative preservation of orbitofrontal cortical volume would imply a proliferation of neurites and neuropil increase. In this respect, the neuropathology of the orbitofrontal cortex in OCD would be intermediate between pathognomonic laminar neurodegeneration in Huntington's disease and probable neuropil hypertrophy with massive gliosis in chorea-acanthocytosis. Scanning of additional hemispheres from new cases with high-resolution MRI scanners (Grinberg et al. 2008) and calculation of post-mortem in cranio volumes of cortical and subcortical regions with stereological volume estimation of the same regions after histological processing and calculation of shrinkage factors and transformation of serial coronal sections into high-resolution virtual sagittal sections for better areal delineation (Alegro et al. 2016; Alho et al. 2018) could be a strategy to solve the question of artifactual or biological volume changes, neuron density, and neuron number differences in controls and age- and sex-matched OCD cases.

The orbitofrontal cortex integrates several sensory modalities including taste, olfaction, pain, auditory, and visual stimuli. These stimuli are associated with learning, memory, emotional, and hedonic aspects. Higher cognitive capacities that depend on these inputs including reward, moral, social judgement, and conduct are obviously arranged in a topographic manner from more medial to more lateral and posterior to anterior aspects (Henssen et al. 2016). The majority of the orbitofrontal areas are covered by a clear-cut six-layered isocortex with increasing width and cell-density of layer IV (Sanides 1962). Pyramidal cells represent about 80% the major cell type of the isocortex. Their layer-wise arrangement reflects connectional/functional aspects of association, commissural, and projection neurons to cortical and subcortical targets (Nieuwenhuys et al. 2008). Layer IV granule cells and layer III pyramidal cells are the main targets of intracortical feed-forward circuits (Pandya and Yeterian 1985). Heavy neuron deficits/loss in orbitofrontal infragranular layers V and VI could be associated with disconnections to accumbens, ventral striatum, pallidum, ventral tegmental area, and extended regions of the substantia nigra pars compacta (Haber et al. 1995). Combined loss of layer III and layer V pyramidal cells could disconnect caudally respectively rostrally directed intraorbital streams whereas intact granule neurons still receive unimpaired cortical somatosensory and visual afferents.

Presently, it is illusive to correlate our findings with resting metabolic state, symptom provocation paradigms,

and pre-post treatment functional neuroimaging studies implicating a hyper-activated OFC pattern in the pathophysiology of OCD (Rauch et al. 1994b; Saxena and Rauch 2000). Findings from structural neuroimaging research have reported OFC volumetric alterations, including both increments and decrements, in OCD patients (Hoexter et al. 2012; Kim et al. 2001; Radua and Mataix-Cols 2009; Rotge et al. 2010; Togao et al. 2010; Valente et al. 2005). Our quantitative data concerning volume differences of OFC areas were subject to histological artifacts and, therefore, are equivocal concerning pathological volume increments of decrements in OCD cases. The majority of cortical pyramidal cells are glutamatergic (Meldrum 2000). Correlation of laminar and region-specific neuron deficits with elevated glutamate and glutamine (Glx/Cr) in the OFC white matter of OCD patients (van de Vondervoort et al. 2016), candidate gene association studies (Mattheisen et al. 2015; Stewart et al. 2013) and the differential expression of the glutamate transporter genes SLC1A1, SLITRK, DLGAP1 and GRIN2B in OCD remain to be established (van de Vondervoort et al. 2016).

The study has some limitations (1) the small sample size, and stereological sampling strategies most likely limited its statistical power to determine significant differences in the total number of neurons. (2) Given the case-control design of post-mortem investigations, it is not possible to determine whether microscopic alterations in the OFC represent a primary site of the disorder, the result of a compensatory mechanism, or an epiphenomenon (3). Our findings are exploratory and, as such, were not adjusted to multiple testing. (4) The subjects were not diagnosed with OCD while alive. To overcome this limitation, we did an extensive post-mortem neuropsychiatric evaluation with the individuals' families to characterize their OCD symptoms. It is worth emphasizing that the post-mortem diagnostic ability of our initial interview was validated (Ferretti et al. 2010). Several of our cases (6) had difficulties in discarding things and a tendency to accumulate possessions; however, all these patients had also one additional obsessive-compulsive symptom. It is worth highlighting that more than 50% of OCD patients had comorbid hoarding symptoms (Torres et al. 2012). Therefore, obtaining well-characterized and diligently processed post-mortem brains from individuals with OCD is a challenge. Future studies should include a higher number and, if possible younger cases with probable OCD.

Acknowledgements This work was supported by Grants no. 2009/51482-0 and 2011/21357-9 provided by the São Paulo Research Foundation (FAPESP) and the National Council of Technological and Scientific Development (CNPq), no. 476647/2010. Kátia Cristina de Oliveira was supported by the Coordination for the Improvement of Higher Education Personnel (CAPES). We are grateful to the families that donated the brains for this study. We would like thank all the members of the Brain Bank of Brazilian Aging Study Group. We would also thank Eduardo Alho MD, PhD for his assistance when using the 3D reconstruction software, the support of the staff from

the Department of Psychiatry, Psychosomatics and Psychotherapy of the Mental Health Center of the University Hospital Würzburg, and the following psychiatrists, who contributed to the OCS diagnosis: E. Serap Monkul, MD, Ricardo Toniolo, MD, Alexandre Gigante, MD, PhD, Ana Gabriela Hounie, MD, Ph.D., Roseli Gedanke Shavitt, MD, Ph.D., Antonio Carlos Lopes, MD, Ph.D., Juliana B Diniz, MD, Ph.D.

Compliance with ethical standards

Conflict of interest The authors report no biomedical financial interests or potential conflicts of interest.


References

- Alegro MAE, Loring B, Heinsen H, Alho E, Zöllei L, Ushizima D, Grinberg LT (2016). Multimodal whole brain registration: MRI and high resolution histology. In: 2016 IEEE conference on computer vision and pattern recognition workshops (CVPRW), pp 634–642
- Alho EJL, Alho ATDL, Grinberg L, Amaro E, Dos Santos GAB, da Silva RE, Neves RC, Alegro M, Coelho DB, Teixeira MJ, Fonoff ET, Heinsen H (2018) High thickness histological sections as alternative to study the three-dimensional microscopic human sub-cortical neuroanatomy. *Brain Struct Funct* 223(3):1121–1132
- Beasley CL, Chana G, Honavar M, Landau S, Everall IP, Cotter D (2005) Evidence for altered neuronal organisation within the planum temporale in major psychiatric disorders. *Schizophr Res* 73(1):69–78
- Beck EA (1949) A cytoarchitectural investigation into the boundaries of cortical areas 13 and 14 in the human brain. *J Anat* 83(2):147–157
- Braak H, Braak E (1991) Neuropathological staging of Alzheimer-related changes. *Acta Neuropathol* 82(4):239–259
- Brodmann K (1909) Vergleichende Lokalisationslehre der Großhirnrinde. Barth, Leipzig
- Chamberlain SR, Menzies L, Hampshire A, Suckling J, Fineberg NA, del Campo N, Aitken M, Craig K, Owen AM, Bullmore ET, Robbins TW, Sahakian BJ (2008) Orbitofrontal dysfunction in patients with obsessive–compulsive disorder and their unaffected relatives. *Science* 321(5887):421–422
- Chiavaras MM, Petrides M (2000) Orbitofrontal sulci of the human and macaque monkey brain. *J Comp Neurol* 422(1):35–54
- Christian CJ, Lencz T, Robinson DG, Burdick KE, Ashtari M, Malhotra AK, Betensky JD, Szeszko PR (2008) Gray matter structural alterations in obsessive–compulsive disorder: relationship to neuropsychological functions. *Psychiatry Res* 164(2):123–131
- Cotter D, Hudson L, Landau S (2005) Evidence for orbitofrontal pathology in bipolar disorder and major depression, but not in schizophrenia. *Bipolar Disord* 7(4):358–369
- de Oliveira KC, Nery FG, Ferretti REL, Lima MC, Cappi C, Machado-Lima A, Polichiso L, Carreira LL, Avila C, Alho ATDL, Brentani HP, Miguel EC, Heinsen H, Jacob-Filho W, Pasqualucci CA, Lafer B, Grinberg LT (2012) Brazilian psychiatric brain bank: a new contribution tool to network studies. *Cell Tissue Bank* 13(2):315–326
- de Wit SJ, Alonso P, Schweren L, Mataix-Cols D, Lochner C, Menchón JM, Stein DJ, Fouché JP, Soriano-Mas C, Sato JR, Hoexter MQ, Denys D, Nakamae T, Nishida S, Kwon JS, Jang JH, Busatto GF, Cardoner N, Cath DC, Fukui K, Jung WH, Kim SN, Miguel EC, Narumoto J, Phillips ML, Pujol J, Remijnse PL, Sakai Y, Shin NY, Yamada K, Veltman DJ, van den Heuvel AO (2014) Multicenter voxel-based morphometry mega-analysis of structural brain scans in obsessive–compulsive disorder. *Am J Psychiatry* 171(3):340–349
- Del-Ben CM, Rodrigues CR, Zuardi AW (1996) Reliability of the Portuguese version of the structured clinical interview for DSM-III-R (SCID) in a Brazilian sample of psychiatric outpatients. *Braz J Med Biol Res* 29(12):1675–1682
- DuPont RL, Rice DP, Shiraki S, Rowland CR (1995) Economic costs of obsessive–compulsive disorder. *Med Interface* 8(4):102–109
- Eberstaller O (1890) Das Stirnhirn. Ein Beitrag zur Anatomie der Oberfläche des Grosshirns. Urban und Schwarzenberg, Leipzig
- Economo CV, Koskinas GN (1925) Die Cytoarchitektonik der Hirnrinde des erwachsenen Menschen. Julius Springer, Berlin
- Einarson L (1932) A Method for Progressive Selective Staining of Nissl and Nuclear Substance in Nerve Cells. *Am J Pathol* 8(3):295–308 295
- Ferretti REL, Damin AE, Brucki SMD, Morillo LS, Perroco TR, Campora F, Moreira EG, Balbino ES, Lima MCAL, Battela C, Ruiz M, Grinberg LT, Farfel JM, Leite REPSCK, Pasqualucci CARSPHJ-FWNR (2010) Post-mortem diagnosis of dementia by informant interview. *Dement Neuropsychol* 4(2):138–144
- First M, Spitzer R, Gibbon M, Williams J (2002) Structured Clinical Interview for DSM-IV-TR Axis I Disorders, Research Version, Patient Edition (SCID-I/P). Psychiatric Institute, New York
- Gillan CM, Apergis-Schoute AM, Morein-Zamir S, Urcelay GP, Sule A, Fineberg NA, Sahakian BJ, Robbins TW (2015) Functional neuroimaging of avoidance habits in obsessive–compulsive disorder. *Am J Psychiatry* 172(3):284–293
- Goodman WK, Price LH, Rasmussen SA, Mazure C, Fleischmann RL, Hill CL, Heninger GR, Charney DS (1989) The Yale–Brown Obsessive Compulsive Scale. I. Development, use, and reliability. *Arch Gen Psychiatry* 46(11):1006–1011
- Grinberg LT, Amaro E, Teipel S, dos Santos DD, Pasqualucci CA, Leite REP, Camargo CR, Goncalves JA, Sanches AG, Santana M, Ferretti REL, Jacob-Filho W, Nitrini R, Heinsen H, Brazilian Aging Brain Study G (2008) Assessment of factors that confound MRI and neuropathological correlation of human postmortem brain tissue. *Cell Tissue Bank* 9(3):195–203
- Haber SN, Kunishio K, Mizobuchi M, Lynd-Balta E (1995) The orbital and medial prefrontal circuit through the primate basal ganglia. *J Neurosci* 15(7 Pt 1):4851–4867
- Harrison BJ, Pujol J, Soriano-Mas C, Hernandez-Ribas R, Lopez-Sola M, Ortiz H, Alonso P, Deus J, Menchon JM, Real E, Segalas C, Contreras-Rodriguez O, Blanco-Hinojo L, Cardoner N (2012) Neural correlates of moral sensitivity in obsessive–compulsive disorder. *Arch Gen Psychiatry* 69(7):741–749
- Heinsen H, Strik M, Bauer M, Luther K, Ulmar G, Gangnus D, Jungkunz G, Eisenmenger W, Gotz M (1994) Cortical and striatal neurone number in Huntington’s disease. *Acta Neuropathol* 88(4):320–333
- Heinsen H, Rub U, Bauer M, Ulmar G, Bethke B, Schuler M, Bocker F, Eisenmenger W, Gotz M, Korr H, Schmitz C (1999) Nerve cell loss in the thalamic mediodorsal nucleus in Huntington’s disease. *Acta Neuropathol* 97(6):613–622
- Henssen A, Zilles K, Palomero-Gallagher N, Schleicher A, Mohlberg H, Gerboga F, Eickhoff SB, Bludau S, Amunts K (2016) Cytoarchitecture and probability maps of the human medial orbitofrontal cortex. *Cortex* 75:87–112
- Hoexter MQ, de Souza Duran FL, D’Alcanta CC, Dougherty DD, Shavitt RG, Lopes AC, Diniz JB, Deckersbach T, Batistuzzo MC, Bressan RA, Miguel EC, Busatto GF (2012) Gray matter volumes in obsessive–compulsive disorder before and after fluoxetine or cognitive-behavior therapy: a randomized clinical trial. *Neuropsychopharmacology* 37(3):734–745
- Hoexter MQ, Diniz JB, Lopes AC, Batistuzzo MC, Shavitt RG, Dougherty DD, Duran FL, Bressan RA, Busatto GF, Miguel EC, Sato JR (2015) Orbitofrontal thickness as a measure for treatment response

- prediction in obsessive–compulsive disorder. *Depression Anxiety* 32(12):900–908
- Hof PR, Mufson EJ, Morrison JH (1995) Human orbitofrontal cortex: cytoarchitecture and quantitative immunohistochemical parcellation. *J Comp Neurol* 359(1):48–68
- Kim JJ, Lee MC, Kim J, Kim IY, Kim SI, Han MH, Chang KH, Kwon JS (2001) Grey matter abnormalities in obsessive–compulsive disorder: statistical parametric mapping of segmented magnetic resonance images. *Br J Psychiatry* 179:330–334
- Kretschmann HJ, Tafesse U, Herrmann A (1982) Different volume changes of cerebral cortex and white matter during histological preparation. *Microsc Acta* 86(1):13–24
- Law AJ, Harrison PJ (2003) The distribution and morphology of prefrontal cortex pyramidal neurons identified using anti-neurofilament antibodies SMI32, N200 and FNP7. Normative data and a comparison in subjects with schizophrenia, bipolar disorder or major depression. *J Psychiatr Res* 37(6):487–499
- Liu J, Heinsen H, Grinberg LT, Alho E, Amaro E, Pasqualucci CA, Rüb U, Seidel K, den Dunnen W, Arzberger T, Schmitz C, Kiessling MC, Bader B, Danek A (2018) Pathoarchitectonics of the cerebral cortex in chorea-acanthocytosis and HD. *Neuropathol Appl Neurobiol*. <https://doi.org/10.1111/nan.12495>
- Mackey S, Petrides M (2010) Quantitative demonstration of comparable architectonic areas within the ventromedial and lateral orbital frontal cortex in the human and the macaque monkey brains. *Eur J Neurosci* 32(11):1940–1950
- Maltby N, Tolin DF, Worhunsky P, O’Keefe TM, Kiehl KA (2005) Dysfunctional action monitoring hyperactivates frontal–striatal circuits in obsessive–compulsive disorder: an event-related fMRI study. *Neuroimage* 24(2):495–503
- Mattheisen M, Samuels JF, Wang Y, Greenberg BD, Fyer AJ, McCracken JT, Geller DA, Murphy DL, Knowles JA, Grados MA, Riddle MA, Rasmussen SA, McLaughlin NC, Nurni EL, Askland KD, Qin HD, Cullen BA, Piacentini J, Pauls DL, Bienvenu OJ, Stewart SE, Liang KY, Goes FS, Maher B, Pulver AE, Shugart YY, Valle D, Lange C, Nestadt G (2015) Genome-wide association study in obsessive–compulsive disorder: results from the OCGAS. *Mol Psychiatry* 20(3):337–344
- Meldrum BS (2000) Glutamate as a neurotransmitter in the brain: review of physiology and pathology. *J Nutr* 130(4S Suppl):1007s–1015s
- Milad MR, Rauch SL (2007) The role of the orbitofrontal cortex in anxiety disorders. *Ann N Y Acad Sci* 1121:546–561
- Milad MR, Rauch SL (2012) Obsessive–compulsive disorder: beyond segregated cortico-striatal pathways. *Trends Cogn Sci* 16(1):43–51
- Mirra SS, Heyman A, McKeel D, Sumi SM, Crain BJ, Brownlee LM, Vogel FS, Hughes JP, van Belle G, Berg L (1991) The Consortium to Establish a Registry for Alzheimer’s Disease (CERAD). Part II. Standardization of the neuropathologic assessment of Alzheimer’s disease. *Neurology* 41(4):479–486
- Murray CJL, Lopez AD (1996) Global burden of disease: a comprehensive assessment of mortality and morbidity from diseases, injuries and risk factors in 1990 and projected to 2020. World Health Organization. Geneva
- Nieuwenhuys R, Voogd J, van Huijzen C (2008) The human central nervous system. Springer, Berlin
- Ongur D, Ferry AT, Price JL (2003) Architectonic subdivision of the human orbital and medial prefrontal cortex. *J Comp Neurol* 460(3):425–449
- Oorschot DE (1994) Are you using neuronal densities, synaptic densities or neurochemical densities as your definitive data? There is a better way to go. *Prog Neurobiol* 44(3):233–247
- Pakkenberg B (1990) Pronounced reduction of total neuron number in mediodorsal thalamic nucleus and nucleus accumbens in schizophrenics. *Arch Gen Psychiatry* 47(11):1023–1028
- Pandya DN, Yeterian EH (1985) Architecture and connections of cortical association areas. In: Peters A, Jones EG (eds) *Cerebral cortex*. Plenum Press, New York, pp 3–61
- Pujol J, Soriano-Mas C, Alonso P, Cardoner N, Menchon JM, Deus J, Vallejo J (2004) Mapping structural brain alterations in obsessive–compulsive disorder. *Arch Gen Psychiatry* 61(7):720–730
- Radua J, Mataix-Cols D (2009) Voxel-wise meta-analysis of grey matter changes in obsessive–compulsive disorder. *Br J Psychiatry* 195(5):393–402
- Rajkowska G, Halaris A, Selemon LD (2001) Reductions in neuronal and glial density characterize the dorsolateral prefrontal cortex in bipolar disorder. *Biol Psychiatry* 49(9):741–752
- Rauch SL, Jenike MA, Alpert NM, Baer L, Breiter HC, Savage CR, Fischman AJ (1994a) Regional cerebral blood flow measured during symptom provocation in obsessive–compulsive disorder using oxygen 15-labeled carbon dioxide and positron emission tomography. *Arch Gen Psychiatry* 51(1):62–70
- Rauch SL, Jenike MA, Alpert NM, Baer L, Breiter HC, Savage CR, Fischman AJ (1994b) Regional cerebral blood flow measured during symptom provocation in obsessive–compulsive disorder using oxygen 15-labeled carbon dioxide and positron emission tomography. *Arch Gen Psychiatry* 51(1):62–70
- Rosario-Campos MC, Miguel EC, Quatrano S, Chacon P, Ferrao Y, Findley D, Katsochis L, Scahill L, King RA, Woody SR, Tolin D, Hollander E, Kano Y, Leckman JF (2006) The Dimensional Yale–Brown Obsessive–Compulsive Scale (DY-BOCS): an instrument for assessing obsessive–compulsive symptom dimensions. *Mol Psychiatry* 11(5):495–504
- Rotge JY, Langbour N, Guehl D, Bioulac B, Jaafari N, Allard M, Aouizerate B, Burbaud P (2010) Gray matter alterations in obsessive–compulsive disorder: an anatomical likelihood estimation meta-analysis. *Neuropsychopharmacology* 35(3):686–691
- Sanides F (1962) Die Architektonik des menschlichen Stirnhirns-Zugleich eine Darstellung der Prinzipien seiner Gestaltung als Spiegel der stammesgeschichtlichen Differenzierung der Grosshirnrinde. In: Müller M, Spatz H, Vogel P (eds) *Monographien aus dem Gesamtgebiete der Neurologie und Psychiatrie*. Springer, Berlin, pp 1–201
- Saxena S, Rauch SL (2000) Functional neuroimaging and the neuroanatomy of obsessive–compulsive disorder. *Psychiatr Clin N Am* 23(3):563–586
- Schmitz C (1997) Towards more readily comprehensible procedures in disector stereology. *J Neurocytol* 26(10):707–710
- Schmitz C (1998) Variation of fractionator estimates and its prediction. *Anat Embryol (Berl)* 198(5):371–397
- Schmitz C (2000) Towards the use of state-of-the-art stereology in experimental gerontology. *Exp Gerontol* 35(3):429–431
- Schmitz C, Hof PR (2000) Recommendations for straightforward and rigorous methods of counting neurons based on a computer simulation approach. *J Chem Neuroanat* 20(1):93–114
- Schmitz C, Hof PR (2005) Design-based stereology in neuroscience. *Neuroscience* 130(4):813–831
- Schmitz C, Korr H, Heinsen H (1999a) Design-based counting techniques: the real problems. *Trends Neurosci* 22(8):345–346
- Schmitz C, Rüb U, Korr H, Heinsen H (1999b) Nerve cell loss in the thalamic mediodorsal nucleus in Huntington’s disease. II. Optimization of a stereological estimation procedure. *Acta Neuropathol* 97(6):623–628
- Spitzer RL, Williams JB, Gibbon M, First MB (1992) The Structured Clinical Interview for DSM-III-R (SCID). I: History, rationale, and description. *Arch Gen Psychiatry* 49(8):624–629
- Stewart SE, Yu D, Scharf JM, Neale BM, Fagerness JA, Mathews CA, Arnold PD, Evans PD, Gamazon ER, Davis LK, Osiecki L, McGrath L, Haddad S, Crane J, Hezel D, Illman C, Mayerfeld C, Konkashbaev A, Liu C, Pluzhnikov A, Tikhomirov A, Edlund CK, Rauch SL, Moessner R, Falkai P, Maier W, Ruhrmann S, Grabe

- HJ, Lennertz L, Wagner M, Bellodi L, Cavallini MC, Richter MA, Cook EH Jr, Kennedy JL, Rosenberg D, Stein DJ, Hemmings SM, Lochner C, Azzam A, Chavira DA, Fournier E, Garrido H, Sheppard B, Umana P, Murphy DL, Wendland JR, Veenstra-VanderWeele J, Denys D, Blom R, Deforce D, Van Nieuwerburgh F, Westenberg HG, Walitza S, Egberts K, Renner T, Miguel EC, Cappi C, Hounie AG, Conceicao do Rosario M, Sampaio AS, Vallada H, Nicolini H, Lanzagorta N, Camarena B, Delorme R, Leboyer M, Pato CN, Pato MT, Voyiaziakis E, Heutink P, Cath DC, Posthuma D, Smit JH, Samuels J, Bienvenu OJ, Cullen B, Fyer AJ, Grados MA, Greenberg BD, McCracken JT, Riddle MA, Wang Y, Coric V, Leckman JF, Bloch M, Pittenger C, Eapen V, Black DW, Ophoff RA, Strengman E, Cusi D, Turiel M, Frau F, Macciardi F, Gibbs JR, Cookson MR, Singleton A, Hardy J, Crenshaw AT, Parkin MA, Mirel DB, Conti DV, Purcell S, Nestadt G, Hanna GL, Jenike MA, Knowles JA, Cox N, Pauls DL (2013) Genome-wide association study of obsessive–compulsive disorder. *Mol Psychiatry* 18(7):788–798
- Stockmeier CA, Mahajan GJ, Konick LC, Overholser JC, Jurjus GJ, Meltzer HY, Uylings HB, Friedman L, Rajkowska G (2004) Cellular changes in the postmortem hippocampus in major depression. *Biol Psychiatry* 56(9):640–650
- Subira M, Cano M, de Wit SJ, Alonso P, Cardoner N, Hoexter MQ, Kwon JS, Nakamae T, Lochner C, Sato JR, Jung WH, Narumoto J, Stein DJ, Pujol J, Mataix-Cols D, Veltman DJ, Menchon JM, van den Heuvel OA, Soriano-Mas C (2016) Structural covariance of neostriatal and limbic regions in patients with obsessive–compulsive disorder. *J Psychiatry Neurosci* 41(2):115–123
- Szeszko PR, Robinson D, Alvir JM, Bilder RM, Lencz T, Ashtari M, Wu H, Bogerts B (1999) Orbital frontal and amygdala volume reductions in obsessive–compulsive disorder. *Arch Gen Psychiatry* 56(10):913–919
- Teachman BA (2007) Linking obsessional beliefs to OCD symptoms in older and younger adults. *Behav Res Ther* 45(7):1671–1681
- Todtenkopf MS, Vincent SL, Benes FM (2005) A cross-study meta-analysis and three-dimensional comparison of cell counting in the anterior cingulate cortex of schizophrenic and bipolar brain. *Schizophr Res* 73(1):79–89
- Togao O, Yoshiura T, Nakao T, Nabeyama M, Sanematsu H, Nakagawa A, Noguchi T, Hiwatashi A, Yamashita K, Nagao E, Kanba S, Honda H (2010) Regional gray and white matter volume abnormalities in obsessive–compulsive disorder: a voxel-based morphometry study. *Psychiatry Res* 184(1):29–37
- Torres AR, Fontenelle LF, Ferrao YA, do Rosario MC, Torresan RC, Miguel EC, Shavitt RG (2012) Clinical features of obsessive–compulsive disorder with hoarding symptoms: a multicenter study. *J Psychiatr Res* 46(6):724–732
- Triarhou LC (2013) The cytoarchitectonic map of Constantin von Economo and Georg N. Koskinas. In: Geyer S, Turner R (eds) *Microstructural parcellation of the human cerebral cortex*. Springer, Berlin
- Uylings HB, Sanz-Arigita EJ, de VK, Pool, Evers CW, Rajkowska P G (2010) 3-D cytoarchitectonic parcellation of human orbitofrontal cortex correlation with postmortem MRI. *Psychiatry Res* 183(1):1–20
- Valente AA Jr, Miguel EC, Castro CC, Amaro E Jr, Duran FL, Buchpiguel CA, Chitnis X, McGuire PK, Busatto GF (2005) Regional gray matter abnormalities in obsessive–compulsive disorder: a voxel-based morphometry study. *Biol Psychiatry* 58(6):479–487
- van de Vondervoort I, Poelmans G, Aschrafi A, Pauls DL, Buitelaar JK, Glennon JC, Franke B (2016) An integrated molecular landscape implicates the regulation of dendritic spine formation through insulin-related signalling in obsessive–compulsive disorder. *J Psychiatry Neurosci* 41(4):280–285
- Vogt C, Vogt O (1919) Allgemeine Ergebnisse unserer Hirnforschung. Dritte Mitteilung. Die architektonische Rindenfelderung im Lichte unserer neuesten Forschungen. *J Psychol Neurol (Lpz)* 25(Ergänzungsheft 1):399–462
- Weibel ER (1979) *Stereological methods*. Academic Press, London
- West MJ (1999) Stereological methods for estimating the total number of neurons and synapses: issues of precision and bias. *Trends Neurosci* 22(2):51–61
- Yoo SY, Roh MS, Choi JS, Kang DH, Ha TH, Lee JM, Kim IY, Kim SI, Kwon JS (2008) Voxel-based morphometry study of gray matter abnormalities in obsessive–compulsive disorder. *J Korean Med Sci* 23(1):24–30

Affiliations

Katia Cristina de Oliveira^{1,2,3,11,13}  · **Lea Tenenholz Grinberg**^{1,12} · **Marcelo Queiroz Hoexter**² · **Helena Brentani**^{6,8,9} · **Claudia Kimie Suemoto**^{1,4} · **Fabiano Gonçalves Nery**³ · **Luzia Carreira Lima**¹ · **Ana Tereza Di Lorenzo Alho**^{1,10,11} · **José Marcelo Farfel**^{1,4} · **Renata Eloah de Lucena Ferretti-Rebustini**^{1,7} · **Renata Elaine Paraizo Leite**^{1,4} · **Ariane Cristine Moretto**^{1,3} · **Alexandre Valotta da Silva**^{1,10} · **Beny Lafer**^{3,9} · **Eurípedes Constantino Miguel**^{2,8,9} · **Ricardo Nitri**^{1,4,5} · **Wilson Jacob-Filho**^{1,4} · **Helmut Heinsen**^{1,11} · **Carlos Augusto Pasqualucci**^{1,13}

¹ Brain Bank of the Brazilian Aging Brain Study Group and HCFMUSP-LIM 22, University of São Paulo Medical School, São Paulo, Brazil

² Program Spectrum Disorders Obsessive–Compulsive Disorder (PROTOC), Department of Psychiatry, University of São Paulo Medical School, São Paulo, Brazil

³ Bipolar Disorder Research Program (PROMAN), Department of Psychiatry, University of São Paulo Medical School, São Paulo, Brazil

⁴ Discipline of Geriatrics, University of São Paulo Medical School, São Paulo, Brazil

⁵ Department of Neurology, University of São Paulo Medical School, São Paulo, Brazil

⁶ LIM 23-Institute of Psychiatry, University of São Paulo Medical School, São Paulo, Brazil

⁷ Medical-Surgical Nursing Department, University of São Paulo School of Nursing, São Paulo, Brazil

⁸ National Institute of Developmental Psychiatry for Children and Adolescents, CNPq São Paulo, São Paulo, Brazil

⁹ Department of Psychiatry, University of São Paulo Medical School, São Paulo, Brazil

¹⁰ Hospital Israelita Albert Einstein, Brain Institute, São Paulo, Brazil

¹¹ Department of Psychiatry, Psychosomatics and Psychotherapy, Mental Health Center, University Hospital Wuerzburg, Würzburg, Germany

¹² Department of Neurology, Memory and Aging Center,
San Francisco, CA, USA

¹³ Departamento de Patologia, Faculdade de Medicina da
Universidade de São Paulo, Av. Dr. Arnaldo, 455, 1° andar,
sala 1353, São Paulo, SP 01246-903, Brazil